Title: Heterosynaptic Plasticity Normalizes Cortical Excitatory-Inhibitory Balance

Authors: Rachel E. Field[1-4]†, James A. D'amour[1-4]†, Robin Tremblay[2,4,5], Bernardo Rudy[2,4,5], and Robert C. Froemke[1-4,6,7]*

Affiliations:

[1] Skirball Institute for Biomolecular Medicine,

[2] Neuroscience Institute,

[3] Department of Otolaryngology,

[4] Department of Neuroscience and Physiology,

[5] Department of Anesthesiology,

New York University School of Medicine, New York, NY, 10016, USA.

[6] Center for Neural Science,

New York University, New York, NY, 10003, USA.

[7] Howard Hughes Medical Institute Faculty Scholar

†: Co-first authorship

* To whom correspondence should be addressed:

Phone: 212-263-4082

Email: robert.froemke@med.nyu.edu

Abstract

Excitation in neural circuits must be carefully controlled by inhibition to regulate information processing and limit over- or under-excitability. During development, inhibitory and excitatory inputs in the cerebral cortex are initially mismatched but become co-tuned, although the mechanisms for balancing inhibition with excitation have remained unknown. Here we show how coordinated long-term synaptic modifications calibrate excitatory and inhibitory synaptic weights across multiple inputs. We simultaneously monitored several inputs onto mouse auditory cortical pyramidal neurons, and induced plasticity at one set of inputs by pairing presynaptic and postsynaptic activity. Changes also occurred at other inputs including heterosynaptic modifications of the largest unpaired excitatory and inhibitory inputs, computed by postsynaptic neurons over a ten-minute period. These distributed changes collectively normalized correlation across synapses, balancing inhibition with excitation. Thus the overall neuronal synaptic weight distribution is monitored on-line, with specific adjustments occurring across multiple inputs to both enhance newly-relevant stimuli while preserving excitability.

One-Sentence Abstract

Heterosynaptic plasticity can rapidly and specifically balance inhibition with excitation across multiple inputs onto cortical pyramidal neurons.

Main Text

In mature cortical networks and elsewhere throughout the adult nervous system, excitation is precisely regulated by a complex set of inhibitory circuits. GABAergic inhibition is important in many features of nervous system function, including spike generation, dendritic integration, synaptic plasticity, sleep, learning and memory, and prevention of pathological activity such as epilepsy (1-5). Consequentially, inhibitory synapses must be carefully calibrated with the relative strengths of excitatory synapses, to ensure that neurons and networks are neither hypo- nor hyper-excitable for prolonged periods. In sensory cortex, this balance between excitation and inhibition seems to be established during early postnatal development (6-11). In particular, frequency tuning curves in the primary auditory cortex (AI) tend to be initially broad or erratic; excitatory inputs mature within the first 1-2 weeks of postnatal life in rodents, but inhibitory tuning requires auditory experience over weeks 2-4 to balance excitation (7,12,13).

Excitatory-inhibitory balance must also be dynamically maintained throughout life, as experience-dependent modification of excitatory synapses (e.g., occurring during and after development, learning, or conditioning) then requires corresponding changes to inhibitory inputs (7,8,14). Network simulation studies supported by experimental data in vitro and in vivo indicate that disruptions of excitatory-inhibitory balance can rapidly produce epileptiform activity and seizures within minutes (1,15-18), meaning that such compensatory mechanisms must act quickly to re-stabilize neural circuits before pathological activity emerges. At least some of these compensatory or homeostatic adjustments take place over hours to days to retain overall cell excitability, as demonstrated in cultured hippocampal and cortical neurons (19-21). Similar homeostatic plasticity and synaptic scaling has been observed in a number of other systems (22), but it remains unclear if these processes would be able to correct for changes in excitability on the

shorter time-scale of activity-dependent plasticity (seconds to minutes), in an input-specific manner required to preserve or promote differential neural computations.

One alternative for regulation of overall excitability is heterosynaptic plasticity, i.e., modifications to other inputs not activated during induction of long-term potentiation (LTP) or other forms of long-term plasticity (14,23-25). Heterosynaptic long-term modifications at specific subsets of monitored inputs have been observed after excitatory LTP at paired 'homosynaptic' sites (7,26-32). However, it is unknown whether inhibitory synapses also undergo heterosynaptic modifications, and how these changes across multiple inputs might be coordinated to improve excitatory-inhibitory balance. Recently, we showed that spike-timing-dependent plasticity (STDP) could be induced at co-activated excitatory and inhibitory synapses (33). Spike pairing induced excitatory and inhibitory LTP, with the degree of inhibitory potentiation depending on the initial amplitude of co-evoked excitatory events. This naturally led to a normalization of the excitation-inhibition ratio at the paired inputs. Here we now ask whether spike pairing also leads to heterosynaptic excitatory and inhibitory modifications, and if these changes might collectively reorganize or enhance the relationship between excitation and inhibition across inputs.

To examine how homosynaptic and heterosynaptic modifications might synergistically affect cortical excitatory-inhibitory balance, we made 115 whole-cell recordings from layer 5 pyramidal neurons in slices of mouse auditory cortex. An array of stimulation electrodes (inter-electrode spacing: 120 µm) was placed in layer 4 and used to sequentially evoke 4-8 sets of excitatory and inhibitory postsynaptic currents (EPSCs and IPSCs) each at a low presentation rate (0.033 Hz) recorded in voltage-clamp (**Fig. 1A**). This form of stimulation recruited separate populations of excitatory and inhibitory presynaptic inputs with a low degree of overlap across channels (**Fig. 1B, fig. S1**), in a manner that mimics the recruitment of thalamocortical inputs onto

cortical neurons in vivo by sensory stimulation (34-37). After measuring baseline synaptic strength for 5-20 minutes, recordings were switched to current-clamp to pair synaptic inputs evoked by one channel of stimulation with postsynaptic spiking induced by depolarization through the whole-cell electrode (33,38,39). Other stimulation channels were not activated during pairing. Following pairing, we resumed sequential stimulation of all channels and monitored paired and unpaired EPSCs and IPSCs for at least 16-25 minutes after pairing.

We found that pairing presynaptic and postsynaptic activity could lead to long-term synaptic modifications at multiple inputs, including inputs that were not activated during the pairing procedure. While some of these changes could be variable from cell to cell, we consistently found that the strongest unpaired excitatory and inhibitory inputs (the 'original best' inputs) were specifically modified minutes after pairing. For example, in the recording shown in **Figure 1C**, repetitively pairing presynaptic activation of channel S4 with postsynaptic spiking (pre→post pairing) induced excitatory and inhibitory LTP at the paired channel (**Fig. 1C**, red symbols; EPSC amplitude indicated by filled circles were increased by 39%, IPSC amplitude indicated by open circles were increased by 51%). These forms of excitatory and inhibitory STDP are similar to our previous study (33). In contrast, the original best unpaired inputs (excitation evoked by channel S3 and inhibition evoked by S2) were both depressed (**Fig. 1C**, blue symbols; EPSCs decreased by –27%, IPSCs decreased by –72%). The other unpaired inputs were not substantially affected on average (**Fig. 1C**, black symbols). Thus spike pairing induces rapid and specific heterosynaptic modifications in addition to more conventional STDP at paired (homosynaptic) inputs.

These selective modifications to the paired and original best inputs acted together to reorganize the overall profile of excitation and inhibition (i.e., 'excitatory-inhibitory balance'). As a metric of excitatory-inhibitory balance, we used the linear correlation coefficient r_{ei} of EPSCs

and IPSCs evoked across stimulation channels. Linear correlation has previously been used to quantify excitatory-inhibitory balance in vivo (7,40-43) and in vitro (44,45). For this example cell, the initial IPSC amplitudes evoked by each of the six channels were mostly unrelated to the strengths of excitation across the stimulation channels (**Fig. 1D**, left, r_{ei}-before: 0.25). This was unsurprising as, *a priori*, excitatory and inhibitory synapses activated by extracellular stimulation need not be functionally related despite spatial proximity near each electrode; note for this recording that the original best EPSCs and IPSCs were evoked by different electrodes. After pairing, however, we observed that this correlation increased, and the amplitudes of excitation and inhibition evoked by each stimulation site were more similar across all monitored channels (**Fig. 1D**, right, r_{ei}-after: 0.48). In other words, after pairing over the six stimulation sites, when EPSCs were smaller IPSCs tended to be smaller, and when EPSCs were larger IPSCs also tended to be larger. This was a consequence of coordinated homosynaptic and heterosynaptic modifications to the paired input (**Fig. 1D**, red arrow) and original best unpaired excitatory and inhibitory inputs (**Fig. 1D**, blue arrowheads). Such activity-dependent changes over multiple paired and unpaired synapses- which collectively act to improve excitatory-inhibitory balance- are reminiscent of similar experience-dependent changes to excitatory and inhibitory synaptic tuning curves in young rodent auditory cortex in vivo (7).

The relative timing of pre/postsynaptic spiking during pairing determined the sign of heterosynaptic plasticity at the originally-strongest inputs. In 25 recordings, we found that pre→post pairing reliably induced LTP at paired excitatory and inhibitory inputs with concomitant heterosynaptic LTD, which was reliably induced at the original best excitatory and inhibitory inputs (**Fig. 2A, fig. S2A, fig. S3A**). While not every cell experienced all four forms of synaptic modifications in absence of changes to other inputs, on average other non-best unpaired inputs

were not consistently modified after pairing (**Fig. 2A**, bottom). In contrast, in 11 other recordings we observed that post→pre pairing induced excitatory LTD and inhibitory LTP as previously reported (33,39), together with heterosynaptic LTP at the original best excitatory and inhibitory inputs (**Fig. 2B, fig. S2B, fig. S3B**). Heterosynaptic excitatory LTP might be useful for compensating for reductions in excitability after homosynaptic LTD at the paired excitatory inputs. Additionally, as pre→post pairing potentiates paired inhibitory inputs, heterosynaptic inhibitory LTD provides a mechanism for bi-directional regulation of inhibitory synaptic strength.

The coordinated synaptic modifications induced by either pre→post or post→pre pairing could affect overall excitatory-inhibitory correlation r_{ei} in similar ways. In general, when this correlation coefficient was initially low (r_{ei}-before <0.4), the correlation was increased after pairing (**Fig. 2C, fig. S2**). This occurred for both pre→post and post→pre pairing (**Fig. 2C**, top; cells to left of red line at r:0.4 are generally above the unity line), indicating that although the specific valence of synaptic modifications might be different, these changes act together to reorganize populations of synaptic inputs and enhance excitatory-inhibitory balance. However, when the excitatory-inhibitory correlation was initially high (r_{ei}-before >0.4), the correlation instead decreased after pairing (**Fig. 2C, fig. S3**). Unpaired inputs receiving only presynaptic spiking via extracellular stimulation showed no long-term change in excitatory-inhibitory correlation (**Fig. 2C**, bottom, gray). Changes in excitatory-inhibitory correlation were due mainly to heterosynaptic modifications of unpaired inputs rather than homosynaptic plasticity of paired inputs, especially when the initial correlation was low. Considered independently, computing r_{ei}-after assuming only changes to paired inputs led to smaller changes than assuming only changes to unpaired inputs (**Fig. 2D**).

Thus pre/post spike pairing rapidly induces heterosynaptic plasticity to effectively normalize excitatory-inhibitory balance, adjusting the relation of inhibition to excitation to promote a moderate level of correlation of ~0.4. This value is close to that observed in vivo in adult rodent auditory cortex after the critical period for tonal frequency tuning (7). Intuitively, when the excitatory-inhibitory correlation was initially low, this was at least in part because the original best excitatory and inhibitory inputs were activated by different channels (in 12/14 pre→post pairing recordings and 5/5 post→pre pairing recordings). Heterosynaptic plasticity at these different inputs would naturally make the best channels more similar, since original best excitation and inhibition were both depressed after pre→post pairing and potentiated after post→pre pairing. Note that when excitatory-inhibitory correlation was initially high, changes to the paired channel also served to normalize the correlation levels; for post→pre pairing, excitation and inhibition were modified in opposite directions.

These findings indicate that single neurons have mechanisms for sensing relative input strengths and communicating this information across diverse excitatory and inhibitory cells, for activity-dependent coordination of overall synaptic strength profiles. Therefore we next aimed to identify such mechanisms and determine how heterosynaptic plasticity was selectively induced at the original best unpaired inputs. We first used two-photon Ca^{2+} imaging to examine dendritic Ca^{2+} events in layer 5 pyramidal cells during pre/post spike pairing (**Fig. 3A**, left). We found that both pre→post and post→pre pairing led to a broadening in backpropagating action potential-evoked Ca^{2+} transients (**Fig. 3A**, 'Normal solution'). We wondered if this enhanced Ca^{2+} signaling triggered by spike pairing was related to the phenomenon of Ca^{2+}-induced Ca^{2+} release from internal stores (46,47). This mechanism could potentially provide a means for intracellular communication across multiple synapses and has been implicated in heterosynaptic modifications

in other temporal lobe structures, including amygdala (30) and hippocampus (48). We found that intracellular perfusion with thapsigargin (to deplete internal calcium stores, 10 µM) prevented this broader Ca^{2+} event, such that transients evoked during pre→post and post→pre pairing were no different than the postsynaptic spike-triggered Ca^{2+} transients alone (**Fig. 3A**, 'Thapsigargin').

Ca^{2+}-induced Ca^{2+} release was also the major mechanism for heterosynaptic plasticity. Either intracellular thapsigargin (**Fig. 3B,C**) or ruthenium red (an antagonist of ryanodine receptors, 20 µM; **Fig. 3C, fig. S4**) prevented heterosynaptic modifications but spared changes to paired excitatory and inhibitory inputs after pre→post or post→pre pairing. In contrast, all changes to paired or unpaired excitatory and inhibitory inputs were prevented by bath application of APV (50 µM) to block NMDA receptors (**Fig. 3C**). Each of these manipulations- thapsigargin, ruthenium red, or APV- prevented significant changes to overall excitatory-inhibitory correlations after spike pairing. Therefore, the intracellular calcium signaling initiated by activation of NMDA receptors at paired excitatory synapses subsequently triggered a set of other modifications, mainly to paired inhibitory synapses and the original best unpaired excitatory and inhibitory synapses.

These results show that heterosynaptic plasticity can be selectively induced at a specific subset of excitatory and inhibitory inputs onto individual postsynaptic neurons. These original best inputs are necessarily locally but not globally maximal, as only a fraction of the total inputs received by these neurons were activated by the stimulation electrode array. As heterosynaptic changes were expressed ~10-20 minutes after pairing, we hypothesized that these locally-maximal inputs were computed by postsynaptic cells within this brief post-pairing period. To test this prediction, we performed a final set of experiments in which multiple inputs were monitored before and after pre/post pairing, as before; however, immediately following pairing, the original best

excitatory and inhibitory inputs (selected to be on the same input channel) were not stimulated for the first ten minutes post-pairing.

In the recording shown in **Figure 4A**, channel 8 evoked the originally-largest EPSCs and IPSCs, channel 6 evoked the second-largest EPSCs and IPSCs, and channel 4 was the paired channel. After pre→post pairing, channel 8 was turned off for ten minutes. During that period, the paired EPSCs and IPSCs increased, while heterosynaptic LTD was induced at the 'relative best' EPSCs and IPSCs evoked by channel 6. When channel 8 was reactivated, the originally largest EPSCs and IPSCs at that channel remained at their initial amplitudes, and were stable until the end of the recording. Over all recordings, the relative best input during the ten-minute post-pairing period was selectively affected by heterosynaptic modifications rather than the original best inputs (**Fig. 4B**). This experiment demonstrates that heterosynaptic plasticity can be specifically manipulated, such that these changes selectively occur at whichever inputs were most strongly activated in a restricted post-pairing period. Furthermore, these results show that cortical neurons have a Ca^{2+}-dependent mechanism for determining and adjusting overall excitation and excitatory-inhibitory balance in a rapid and stimulus-specific manner.

Here we have described how organized forms of long-term homosynaptic and heterosynaptic plasticity selectively adjust populations of excitatory and inhibitory inputs onto mouse cortical pyramidal neurons. Although inputs evoked by each stimulation channel may not initially be functionally related, these inputs become bound together via repetitive co-activation together with postsynaptic spiking. This might emulate how novel sensory stimuli recruit initially-unrelated inputs, which become functionally coupled via mechanisms of experience-dependent plasticity. Part of this mechanism involves computing local maxima of incoming inputs for selective modifications of specific synapses. Combined with slower forms of homeostatic

plasticity (22), individual cortical neurons have the capability to integrate or accumulate recent activity over minutes to hours, enabling flexible representations of external stimuli and control over excitability on multiple short and long time-scales.

Although excitatory-inhibitory balance is a fundamental feature of neural networks (10,14,40,45), it has remained unclear how this organization is set up and calibrated on-line, especially in response to changes of excitatory synapses believed to be important for learning and memory storage. Instead of a rapid, global optimization process- which might be difficult to biologically implement- our results demonstrate that a restricted set of activity-dependent changes is sufficient to normalize excitatory-inhibitory balance within minutes, enhancing the relation between inhibition and excitation when mismatched, or reducing this value if inhibition is too restrictive. Consequentially, heterosynaptic plasticity and inhibitory plasticity work together to automatically restructure excitatory-inhibitory balance after induction of long-term excitatory modifications to update information storage without disrupting overall network function.

References and Notes

1. Cossart, R., Dinocourt, C., Hirsch, J.C., Merchan-Perez, A., De Felipe, J., Ben-Ari, Y., Esclapez, M., and Bernard, C. (2001). Dendritic but not somatic GABAergic inhibition is decreased in experimental epilepsy. Nat. Neurosci. *4*, 52-62.
2. Isaacson, J.S., and Scanziani, M. (2011). How inhibition shapes cortical activity. Neuron *72*, 231-243.
3. Oliveira, M.S., Pacheco, L.F., Mello, C.F., Cavalheiro, E.A., and Garrido-Sanabria, E.R. (2011). Epileptiform activity in the limbic system. Front. Biosci. *3*, 565-593.
4. Scharfman, H.E., and Brooks-Kayal, A.R. (2014). Is plasticity of GABAergic mechanisms relevant to epileptogenesis? Adv. Exp. Med. Biol. *813*, 133-150.
5. Hattori, R., Kuchibhotla, K., Froemke, R.C., and Komiyama, T. (2017). Modulation and plasticity of inhibition. Nat. Neurosci. *20*, 1199-1208.
6. Gandhi, S.P., Yanagawa, Y., and Stryker, M.P. (2008). Delayed plasticity of inhibitory neurons in developing visual cortex. Proc. Natl. Acad. Sci. U S A. *105*, 16797-16802.
7. Dorrn, A.L., Yuan, K., Barker, A.J., Schreiner, C.E., and Froemke, R.C. (2010). Developmental sensory experience balances cortical excitation and inhibition. Nature *465*, 932-936.
8. House, D.R.C., Elstrott, J., Koh, E., Chung, J., and Feldman, D.E. (2011). Parallel regulation of feedforward inhibition and excitation during whisker map plasticity. Neuron *72*, 819-831.
9. Kuhlman, S.J., Olivas, N.D., Tring, E., Ikrar, T., Xu, X., and Trachtenberg, J.T. (2013). A disinhibitory microcircuit initiates critical-period plasticity in the visual cortex. Nature *501*, 543-546.
10. Takesian, A.E., and Hensch, T.K. (2013). Balancing plasticity/stability across brain development. Prog Brain Res. *207*, 3-34.

11. Cai, D., *et al*. (2017). A critical role of inhibition in temporal processing maturation in the primary auditory cortex. Cereb. Cortex in press.
12. Chang, E.F., Bao, S., Imaizumi, K., Schreiner, C.E., and Merzenich, M.M. (2005). Development of spectral and temporal response selectivity in the auditory cortex. Proc. Natl. Acad. Sci. U.S.A. *102*, 16460-16465.
13. de Villers-Sidani, E., Chang, E.F., Bao, S., and Merzenich, M.M. (2007). Critical period window for spectral tuning defined in the primary auditory cortex (A1) in the rat. J. Neurosci. *27*, 180-189.
14. Froemke, R.C. (2015). Plasticity of cortical excitatory-inhibitory balance. Annu. Rev. Neurosci. *38*, 195-219.
15. Toader, O., Forte, N., Orlando, M., Ferrea, E., Raimondi, A., Baldelli, P., Benfenati, F., and Medrihan, L. (2013). Dentate gyrus network dysfunctions precede the symptomatic phase in a genetic mouse model of seizures. Front. Cell. Neurosci. *7*, 138.
16. Ren, H., Shi, Y.J., Lu, Q.C., Liang, P.J., and Zhang, P.M. (2014). The role of the entorhinal cortex in epileptiform activities of the hippocampus. Theor. Biol. Med. Model. *11*, 14.
17. Avoli, M., de Curtis, M., Gnatkovsky, V., Gotman, J., Köhling, R., Lévesque, M., Manseau, F., Shiri, Z., and Williams, S. (2016). Specific imbalance of excitatory/inhibitory signaling establishes seizure onset pattern in temporal lobe epilepsy. J. Neurophysiol. *115*, 3229-3237.
18. Dehghani, N., Peyrache, A., Telenczuk, B., Le Van Quyen, M., Halgren, E., Cash, S.S., Hatsopoulos, N.G., and Destexhe, A. (2016). Dynamic balance of excitation and inhibition in human and monkey neocortex. Sci. Rep. *6*, 23176.
19. Lissin, D.V., Gomperts, S.N., Carroll, R.C., Christine, C.W., Kalman, D., Kitamura, M., Hardy, S., Nicoll, R.A., Malenka, R.C., and von Zastrow, M. (1998). Activity differentially

regulates the surface expression of synaptic AMPA and NMDA glutamate receptors. Proc. Natl. Acad. Sci. U S A *95*, 7097-7102.

20. Turrigiano, G.G., Leslie, K.R., Desai, N.S., Rutherford, L.C., and Nelson, S.B. (1998). Activity-dependent scaling of quantal amplitude in neocortical neurons. Nature *391*, 892-896.
21. Thiagarajan, T.C., Lindskog, M., and Tsien, R.W. (2005). Adaptation to synaptic inactivity in hippocampal neurons. Neuron *47*, 725-737.
22. Turrigiano, G.G. (2008) The self-tuning neuron: synaptic scaling of excitatory synapses. Cell 135, 422-435.
23. Chistiakova, M., Bannon, N.M., Chen, J.Y., Bazhenov, M., and Volgushev, M. (2015). Homeostatic role of heterosynaptic plasticity: models and experiments. Front. Comput. Neurosci. *9*, 89.
24. Hiratani, N., and Fukai, T. (2017). Detailed dendritic excitatory/inhibitory balance through heterosynaptic spike-timing-dependent plasticity. J. Neurosci. *37*, 12106-12122.
25. Zenke, F., Gerstner, W., and Ganguli, S. (2017). The temporal paradox of Hebbian learning and homeostatic plasticity. Curr. Opin. Neurobiol. *43*, 166-176.
26. Lynch, G.S., Dunwiddie, T., and Gribkoff, V. (1977). Heterosynaptic depression: a postsynaptic correlate of long-term potentiation. Nature *266*, 737-739.
27. Christie, B.R., and Abraham, W.C. (1992). NMDA-dependent heterosynaptic long-term depression in the dentate gyrus of anaesthetized rats. Synapse *10*, 1-6.
28. Muller, D., Hefft, S., and Figurov, A. (1995). Heterosynaptic interactions between LTP and LTD in CA1 hippocampal slices. Neuron *14*, 599-605.
29. Scanziani, M., Malenka, R.C., and Nicoll, R.A. (1997). Role of intercellular interactions in heterosynaptic long-term depression. Nature *380*, 446-450.

30. Royer, S., and Pare, D. (2003). Conservation of total synaptic weight through balanced synaptic potentiation and depression. Nature *422*, 518-522.

31. Froemke, R.C., Carcea, I., Barker, A.J., Yuan, K., Seybold, B.A., Martins, A.R., Zaika, N., Bernstein, H., Wachs, M., Levis, P.A., Polley, D.B., Merzenich, M.M., and Schreiner, C.E. (2013). Long-term modification of cortical synapses improves sensory perception. Nat. Neurosci. *16*, 79-88.

32. Basu, J., Zaremba, J.D., Cheung, S.K., Hitti, F.L., Zemelman, B.V., Losonczy, A., and Siegelbaum, S.A. (2016). Gating of hippocampal activity, plasticity, and memory by entorhinal cortex long-range inhibition. Science *351*, aaa5694.

33. D'amour, J.A., and Froemke, R.C. (2015). Inhibitory and excitatory spike-timing-dependent plasticity in the auditory cortex. Neuron *86*, 514-528.

34. Miller, L.M., Escabí, M.A., Read, H.L., and Schreiner, C.E. (2001). Functional convergence of response properties in the auditory thalamocortical system. Neuron *32*, 151-160.

35. Lee, C.C., Imaizumi, K., Schreiner, C.E., and Winer, J.A. (2004). Concurrent tonotopic processing streams in auditory cortex. Cereb. Cortex *14*, 441-451.

36. Froemke, R.C., Merzenich, M.M., and Schreiner, C.E. (2007). A synaptic memory trace for cortical receptive field plasticity. Nature *450*, 425-429.

37. Hackett, T.A., Barkat, T.R., O'Brien, B.M., Hensch, T.K., and Polley, D.B. Linking topography to tonotopy in the mouse auditory thalamocortical circuit. J. Neurosci. *31*, 2983-2995.

38. Bi, G.Q., and Poo, M.M. (1998). Synaptic modifications in cultured hippocampal neurons: dependence on spike timing, synaptic strength, and postsynaptic cell type. J. Neurosci. *18*, 10464-10472.

39. Feldman, D.E. (2000). Timing-based LTP and LTD at vertical inputs to layer II/III pyramidal cells in rat barrel cortex. Neuron *27*, 45-56.

40. Wehr, M. and Zador, A. M. (2003). Balanced inhibition underlies tuning and sharpens spike timing in auditory cortex. Nature *426*, 442-446.

41. Higley, M.J., and Contreras, D. (2006). Balanced excitation and inhibition determine spike timing during frequency adaptation. J. Neurosci. *26*, 448-457.

42. Okun, M., and Lampl, I. (2008). Instantaneous correlation of excitation and inhibition during ongoing and sensory-evoked activities. Nat. Neurosci., *11*, 535-537.

43. Tan, A.Y., and Wehr, M. (2009). Balanced tone-evoked synaptic excitation and inhibition in mouse auditory cortex. Neuroscience *163*, 1302-1315.

44. Graupner, M., and Reyes, A.D. (2013). Synaptic input correlations leading to membrane potential decorrelation of spontaneous activity in cortex. J. Neurosci. *33*, 15075-15085.

45. Xue, M., Atallah, B.V., and Scanziani, M. (2014). Equalizing excitation-inhibition ratios across visual cortical neurons. Nature *511*, 596-600.

46. Larkum, M.E., Watanabe, S., Nakamura, T., Lasser-Ross, N., and Ross, W.N. (2003). Synaptically activated Ca2+ waves in layer 2/3 and layer 5 rat neocortical pyramidal neurons. J. Physiol. 549, 471-488.

47. Lee, K.F.H., Soares, C., Thiverge, J.-P., and Beique, J.-C. (2016). Correlated synaptic inputs drive dendritic calcium amplification and cooperative plasticity during clustered synapse development. Neuron *89*, 784-799.

48. Nishiyama, M., Hong, K., Mikoshiba, K., Poo, M.-M., and Kato, K. (2000). Calcium stores regulate the polarity and input specificity of synaptic modification. Nature 408, 584-588.

Acknowledgements:

We thank K. Kuchibhotla, M. Jin, E. Morina, D. Talos, and N. Zaika for comments, discussions, and technical assistance. This work was funded by grants from NIDCD (DC009635 and DC012557), a Sloan Research Fellowship, a Klingenstein Fellowship, and a Howard Hughes Medical Institute Faculty Scholarship to R.C.F.

Author Contributions:

All authors designed the studies and wrote the paper. R.E Field, J.A. D'amour, and R. Tremblay performed the experiments and analyzed the data.

Figure Legends

Figure 1. Spike pairing induces modifications of excitation and inhibition at paired and unpaired inputs.

(**A**) Whole-cell recordings from mouse auditory cortical layer 5 pyramidal cells in brain slices containing 8-electrode stimulation array (channels S1-S8) placed in layer 4. Scale, 250 µm.

(**B**) Left, recordings made in voltage-clamp to measure baseline and post-pairing EPSCs at –70 mV (black) and IPSCs at –30 mV (gray). Note that the amplitude of IPSCs do not necessarily scale with the amplitude of EPSCs evoked from the same channel. Scale: 500 msec, 200 pA. Pairing performed in current-clamp. Right, input summation testing, measuring inputs S3, S4, S5 separately and together; predicted summed response compared to measured summed response. Scale: 50 msec, 100 pA.

(**C**) Synaptic strength of multiple excitatory (left) and inhibitory inputs (right) onto the same neuron before and after pairing one channel with postsynaptic spiking. Top, example of excitatory and inhibitory plasticity induced by pre→post pairing at channel S4 (red, Δt: 0.5 msec; EPSCs before pairing: –77.4±7.4 pA; EPSCs after pairing: –107.5±6.1 pA, increase of 38.9%; IPSCs before pairing: 18.4±2.8 pA; IPSCs after pairing: 27.7±2.4 pA, increase of 50.6%). Dashed line, pre-pairing mean. Upper middle, heterosynaptic LTD at the strongest unpaired inputs onto this cell (blue, EPSCs at best channel S3 before: –254.0±12.3 pA, EPSCs after: –185.2±11.2 pA, decrease of –27.1%; IPSCs at best channel S2 before: 150.3±37.0 pA, IPSCs after: 41.4±10.1 pA, decrease of –72.4%). Lower middle, examples showing little change to other inputs (black, EPSCs at channel S6 before: –71.2±5.1 pA, EPSCs after: –80.7±6.9 pA, increase of 13.3%; IPSCs at channel S3 before: 37.9±8.2 pA, IPSCs after: 36.7±10.1 pA, decrease of –3.3%). Bottom, series and input

resistances were stable (Rs before: 14.9±0.4 MΩ, Rs after: 12.4±0.1 MΩ, decrease of −16.2%; Ri before: 136.0±0.7 MΩ, Ri after: 134.6±0.8 MΩ, decrease of −1.0%).

(**D**) Improvement in excitatory-inhibitory balance after spike pairing at one channel; same cell as **C**. Excitatory-inhibitory correlation before pairing (r_{ei}-before, dashed lines) and after pairing (r_{ei}-after, solid lines). Spike pairing at a single channel led to long-lasting increase in excitatory-inhibitory correlation across all channels (r_{ei}-before: 0.25; r_{ei}-after: 0.48). Red arrow, paired channel. Blue arrowheads, original best excitation (filled) and inhibition (open). Error bars represent s.e.m.

Figure 2. Heterosynaptic plasticity normalizes excitatory-inhibitory correlations.

(**A**) Summary of pre→post experiments on paired (top, red; paired EPSCs increased by 40.3±10.5% at 16-25 minutes post-pairing, n=25, $p<0.0009$, Student's paired two-tailed t-test, 18/25 cells showed significant excitatory LTP; paired IPSCs increased by 53.7±13.9%, $p<0.0008$, 19/25 cells showed significant inhibitory LTP), original best (middle, blue; originally-largest EPSCs decreased by −21.7±4.1% at 16-25 minutes post-pairing, $p<10^{-4}$, 21/25 cells showed significant heterosynaptic excitatory LTD; originally-largest IPSCs decreased by −15.4±6.0%, $p<0.02$, 16/25 cells showed significant heterosynaptic inhibitory LTD), and other unpaired inputs (bottom, black; EPSCs increased by 1.4±8.0% at 16-25 minutes post-pairing, $p>0.8$; IPSCs increased by 0.7±4.6%, $p>0.8$). Filled symbols, excitation; open symbols, inhibition.

(**B**) Summary of post→pre pairing experiments on paired (top, red; paired EPSCs decreased by −17.0±6.4% at 16-25 minutes post-pairing, n=11, $p<0.03$, 9/11 cells showed significant excitatory LTD; paired IPSCs increased by 37.9±12.4%, $p<0.02$, 8/11 cells showed significant inhibitory LTP), original best (middle, blue; originally-largest EPSCs increased by 15.6±4.4% at 16-25

minutes post-pairing, $p<0.006$, 7/11 cells showed significant heterosynaptic excitatory LTP; originally-largest IPSCs increased by 25.1±8.6%, $p<0.02$, 7/11 cells showed significant heterosynaptic inhibitory LTP), and other unpaired inputs (bottom, black; EPSCs increased by 4.1±5.1% at 16-25 minutes post-pairing, $p>0.4$; IPSCs increased by 2.7±11.5%, $p>0.8$).

(**C**) Normalization of excitatory-inhibitory correlation after spike pairing. Top, excitatory-inhibitory correlation before (r_{ei}-before) and after (r_{ei}-after) pre→post pairing (left, n=25) or post→pre pairing (n=11). Red vertical line indicates r_{ei}:0.4. Bottom, summary of changes in excitatory-inhibitory linear correlation coefficient after pairing (Δr_{ei}; when initially $r<0.4$ for pre→post pairing: 0.30±0.06, n=14, $p<0.0005$, and for post→pre pairing: 0.11±0.03, n=5, $p<0.02$; when initially $r>0.4$ for pre→post pairing: –0.29±0.13, n=11, $p<0.05$, and for post→pre pairing: –0.13±0.05, n=6, $p<0.05$; and for control cells without pre/postsynaptic paired spiking: –0.04±0.3, n=4, $p>0.2$; Student's paired two-tailed t-test).

(**D**) Heterosynaptic modifications to unpaired inputs played a predominant role in refinement of excitatory-inhibitory balance across channels. Considered separately, increases in synaptic strength only at the paired synapses were less effective by themselves at normalizing the correlation between excitation and inhibition ("Paired only", change in linear correlation coefficient Δr_{ei} when initially $r<0.4$ for pre→post pairing: 0.07±0.06, n=14, $p>0.2$, and for post→pre pairing: –0.08±0.08, n=5, $p>0.3$; and when initially $r>0.4$ for pre→post pairing: –0.20±0.11, n=11, $p>0.1$, and for post→pre pairing: –0.10±0.08, n=6, $p>0.2$; Student's paired two-tailed t-test) than changes to other inputs ("Unpaired only", change in linear correlation coefficient Δr_{ei} when initially $r<0.4$ for pre→post pairing: 0.24±0.07, $p<0.005$, and for post→pre pairing: 0.13±0.02, $p<0.005$; and when initially $r>0.4$ for pre→post pairing: –0.27±0.09, $p<0.02$,

but not for post→pre pairing: –0.06±0.05, $p>0.2$). *, $p<0.05$; **, $p<0.01$. Error bars represent s.e.m.

Figure 3. Mechanisms of input-specific heterosynaptic plasticity.

(**A**) Spike pairing leads to release of dendritic Ca^{2+} from internal stores. Left, example of two-photon imaging of pairing-induced Ca^{2+} signals in apical dendrites of layer 5 pyramidal neurons; dashed box, analysis region. Middle, examples of Ca^{2+} transients evoked by single postsynaptic spikes (black dashed line) and postsynaptic spikes paired with presynaptic stimulation (black solid line). Shown are single exponential fits to each transient (thin gray lines). Thapsigargin included in the whole-cell pipette prevented the broadening of dendritic Ca^{2+} after both pre→post pairing and post→pre pairing. Right, summary of pairing-induced Ca^{2+} release quantified by time constant τ of single exponential fits. With normal intracellular solution, pairing broadened the evoked Ca2+ signals for both pre→post pairing (top, postsynaptic spike alone, τ: 155.2±29.9 msec; pairing, τ: 295.3±60.6 msec, n=7, $p<0.04$) and post→pre pairing (bottom, postsynaptic spike alone, τ: 164.1±40.4 msec; pairing, τ: 324.9±92.9 msec, n=7, $p<0.04$). This Ca^{2+} event was prevented by thapsigargin in the internal solution (pre→post pairing, postsynaptic spike alone, τ: 191.6±46.5 msec; pairing, τ: 203.6±43.1 msec, n=4, $p>0.4$; post→pre pairing, postsynaptic spike alone, τ: 244.7±34.6 msec; pairing, τ: 229.7±34.1 msec, n=3, $p>0.1$).

(**B**) Thapsigargin in the whole-cell pipette (20 μM) prevents heterosynaptic excitatory and inhibitory LTD after pre→post pairing. Top, example of excitatory LTP (left) and inhibitory LTP (right) induced by pre→post pairing at channel S4 (red, Δt=4 msec; EPSCs before pairing: –100.5±6.5 pA, EPSCs after pairing: –119.0±3.4 pA, increase of 18.3%; IPSCs before pairing: 64.5±4.2 pA, IPSCs after pairing: 100.5±3.6 pA, increase of 55.8%). Dashed line, pre-pairing

mean. Middle, thapsigargin prevented heterosynaptic LTD at the strongest unpaired inputs onto this cell (blue, EPSCs at channel S7 before: –283.9±5.1 pA, EPSCs after: –280.7±15.4 pA, decrease of –1.1%; IPSCs at channel S7 before: 160.4±4.9 pA, IPSCs after: 195.3±9.1 pA, increase of 21.8%). Bottom, series and input resistance were stable (Rs before: 32.4±0.3 MΩ, Rs after: 26.5±0.2 MΩ, decrease of –18.2%; Ri before: 280.7±13.0 MΩ, Ri after: 268.1±7.9 MΩ, decrease of –4.5%).

(**C**) Summary of pharmacological studies. Upper left, effects of pre→post and post→pre pairing with normal intracellular solution and ACSF on paired (red), original best unpaired (blue) and other unpaired inputs (black); same recordings as **Figure 2A,B**. Filled bars, excitation; open bars, inhibition.

Upper right, blocking NMDA receptors with APV in the bath (50 µm) prevented homosynaptic and heterosynaptic plasticity of both excitation and inhibition (pre→post pairing: paired EPSCs decreased by –0.9±3.3% n=6, p>0.7, Student's paired two-tailed t-test; paired IPSCs increased by 5.3±6.3%, p>0.4; originally-largest unpaired EPSCs decreased by –3.1±5.6%, p>0.6; originally-largest unpaired IPSCs increased by 4.9±7.3%, p>0.5; other unpaired EPSCs decreased by –3.8±4.9%, p>0.4; other unpaired IPSCs increased by 3.8±6.7%, p>0.5; post→pre pairing: paired EPSCs increased by 2.8±10.4% n=4, p>0.8; paired IPSCs increased by 1.3±3.2%, p>0.7; originally-largest unpaired EPSCs decreased by –4.1±7.1%, p>0.6; originally-largest unpaired IPSCs increased by 4.2±6.8%, p>0.5; other unpaired EPSCs increased by 1.2±8.7%, p>0.9; other unpaired IPSCs decreased by –0.3±1.5%, p>0.8).

Lower left, intracellular perfusion with ruthenium red (20 µm) spared homosynaptic plasticity at paired inputs but prevented heterosynaptic plasticity at the original best excitation and inhibition (pre→post pairing, n=9: paired EPSCs increased by 18.2±5.0%, p<0.02; paired IPSCs

increased by 41.4±15.6%, $p<0.05$; originally-largest unpaired EPSCs increased by 1.4±4.0%, $p>0.6$; originally-largest unpaired IPSCs increased by 10.0±8.5%, $p>0.3$; other unpaired EPSCs decreased by –9.0±3.9%, $p>0.1$; other unpaired IPSCs increased by 5.3±5.0%, $p>0.3$; post→pre pairing, n=9: paired EPSCs decreased by –18.3±4.6%, $p<0.004$; paired IPSCs increased by 34.2±9.2%, $p<0.006$; originally-largest unpaired EPSCs increased by 0.3±4.4%, $p>0.9$; originally-largest unpaired IPSCs increased by 3.6±7.6%, $p>0.6$; other unpaired EPSCs decreased by –5.7±2.2%, $p>0.05$; other unpaired IPSCs increased by 12.0±6.4%, $p>0.1$).

Lower right, intracellular perfusion with thapsigargin (10 µm) spared homosynaptic plasticity but prevented heterosynaptic plasticity (pre→post pairing, n=12: paired EPSCs increased by 15.9±4.3%, $p<0.006$; paired IPSCs increased by 38.8±9.7%, $p<0.003$; originally-largest unpaired EPSCs decreased by –2.4±1.1%, $p>0.05$; originally-largest unpaired IPSCs increased by 8.7±4.8%, $p>0.1$; other unpaired EPSCs decreased by –4.3±2.3%, $p>0.1$; other unpaired IPSCs increased by 1.1±4.6%, $p>0.8$; post→pre pairing, n=10: paired EPSCs decreased by –21.5±6.5%, $p<0.01$; paired IPSCs increased by 26.7±7.5%, $p<0.006$; originally-largest unpaired EPSCs decreased by –3.5±1.3%, $p>0.05$; originally-largest unpaired IPSCs decreased by –5.5±4.4%, $p>0.2$; other unpaired EPSCs decreased by –5.1±4.2%, $p>0.2$; other unpaired IPSCs decreased by –0.2±5.1%, $p>0.9$).

Figure 4. Postsynaptic neurons compute maximally strong inputs for heterosynaptic plasticity in a ten-minute period following induction of homosynaptic modifications.

(**A**) Deactivating original best input channel led to heterosynaptic excitatory and inhibitory LTD at the second best ('relative best') channel after pre→post pairing. Top, example of excitatory LTP (left) and inhibitory LTP (right) induced by pre→post pairing at channel S4 (red, Δt=4 msec;

EPSCs before pairing: –80.7±3.9 pA, EPSCs after pairing: –90.7±4.7 pA, increase of 12.4%; IPSCs before pairing: 58.0±1.4 pA, IPSCs after pairing: 77.0±1.7 pA, increase of 32.9%). Dashed line, pre-pairing mean. Upper middle, original best inputs evoked by S8 were unaltered when this channel was turned off for ten minutes immediately after pairing (dark blue, original best EPSCs before: –175.6±5.7 pA, original best EPSCs after: –168.6±3.1 pA, decrease of –4.0%; original best IPSCs before: 146.3±10.1 pA, original best IPSCs after: 146.8±5.2 pA, increase of 1.0%). Lower middle, heterosynaptic depression was induced at the relative best inputs evoked by S6 (light blue, relative best EPSCs before: –143.6±5.6 pA, relative best EPSCs after: –114.4±2.5 pA, decrease of –20.3%; relative best IPSCs before: 73.7±5.0 pA, relative best IPSCs after: 52.9±5.4 pA, decrease of –28.3%). Bottom, series and input resistance (Rs before: 15.1±0.1 MΩ, Rs after: 19.5±0.2 MΩ, increase of 28.7%; Ri before: 199.2±1.9 MΩ, Ri after: 169.6±0.7 MΩ, decrease of –14.8%).

(**B**) Summary of pre→post experiments with original best input channel deactivated for the ten-minute post-pairing period. Shown are changes to paired inputs (red; paired EPSCs increased by 22.7±8.4% at 16-25 minutes post-pairing, n=8, $p<0.04$, Student's paired two-tailed t-test; paired IPSCs increased by 19.8±6.0%, $p<0.02$), original best inputs (dark blue; originally-largest EPSCs increased by 2.8±5.6% at 16-25 minutes post-pairing, $p>0.6$; originally-largest IPSCs increased by 9.0±12.1%, $p>0.4$), relative best inputs (light blue; EPSCs decreased by –20.6±4.8% at 16-25 minutes post-pairing, $p<0.004$; IPSCs decreased by –18.2±4.4%, $p<0.02$), and averaged other inputs (black; EPSCs increased by 1.6±9.2% at 16-25 minutes post-pairing, $p>0.8$; IPSCs decreased by –0.5±6.6%, $p>0.9$). Filled symbols, excitation; open symbols, inhibition.

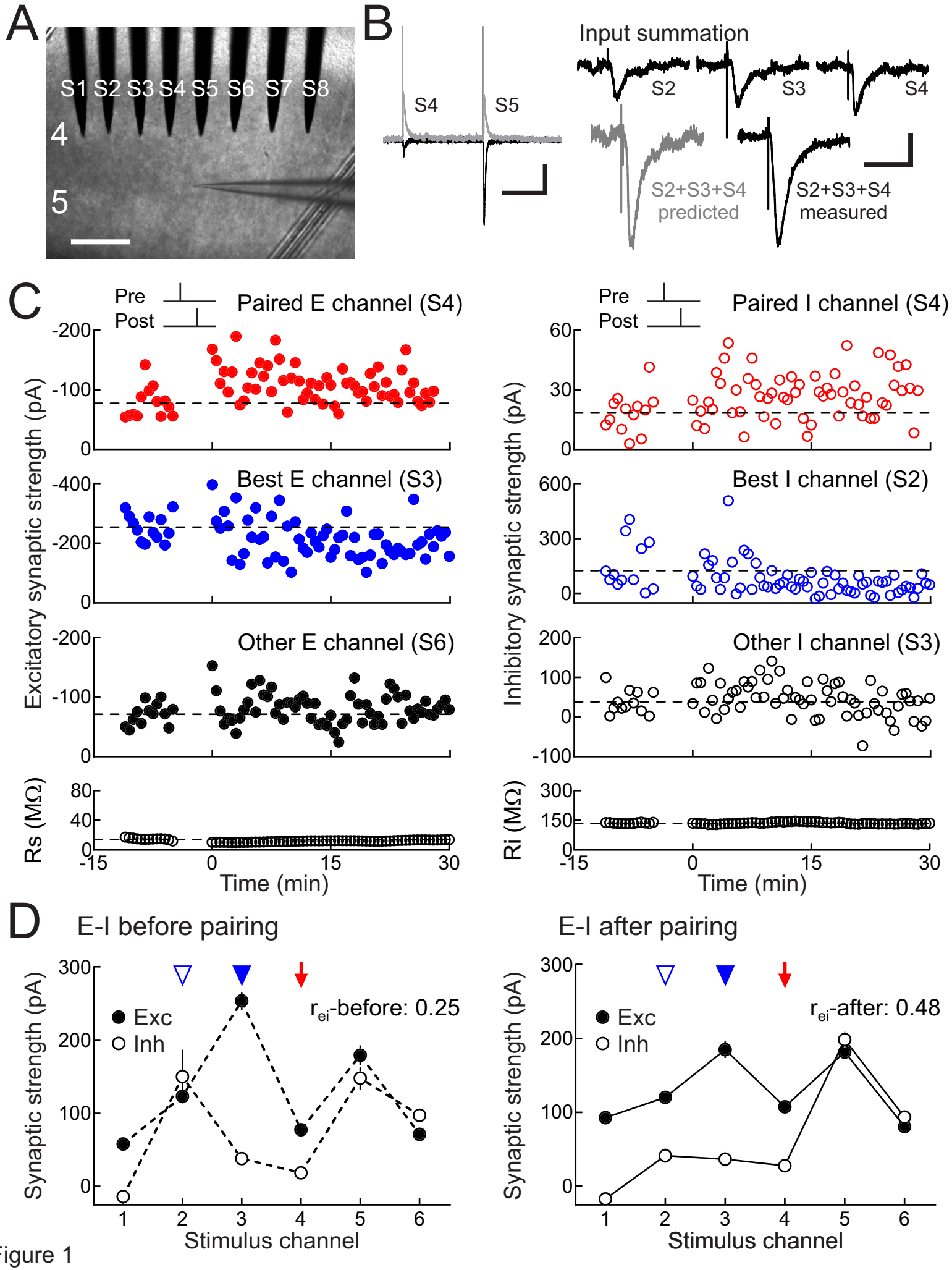
A
S1 S2 S3 S4 S5 S6 S7 S8
4
5
B
S4
S5
Input summation
S2
S3
S4
S2+S3+S4
predicted
S2+S3+S4
measured
C
Pre
Post
Paired E channel (S4)
Best E channel (S3)
Other E channel (S6)
Excitatory synaptic strength (pA)
Rs (MΩ)
Time (min)
Paired I channel (S4)
Best I channel (S2)
Other I channel (S3)
Inhibitory synaptic strength (pA)
Ri (MΩ)
Time (min)
D
E-I before pairing
E-I after pairing
Exc
Inh
r_{ei}-before: 0.25
r_{ei}-after: 0.48
Synaptic strength (pA)
Stimulus channel

Figure 1

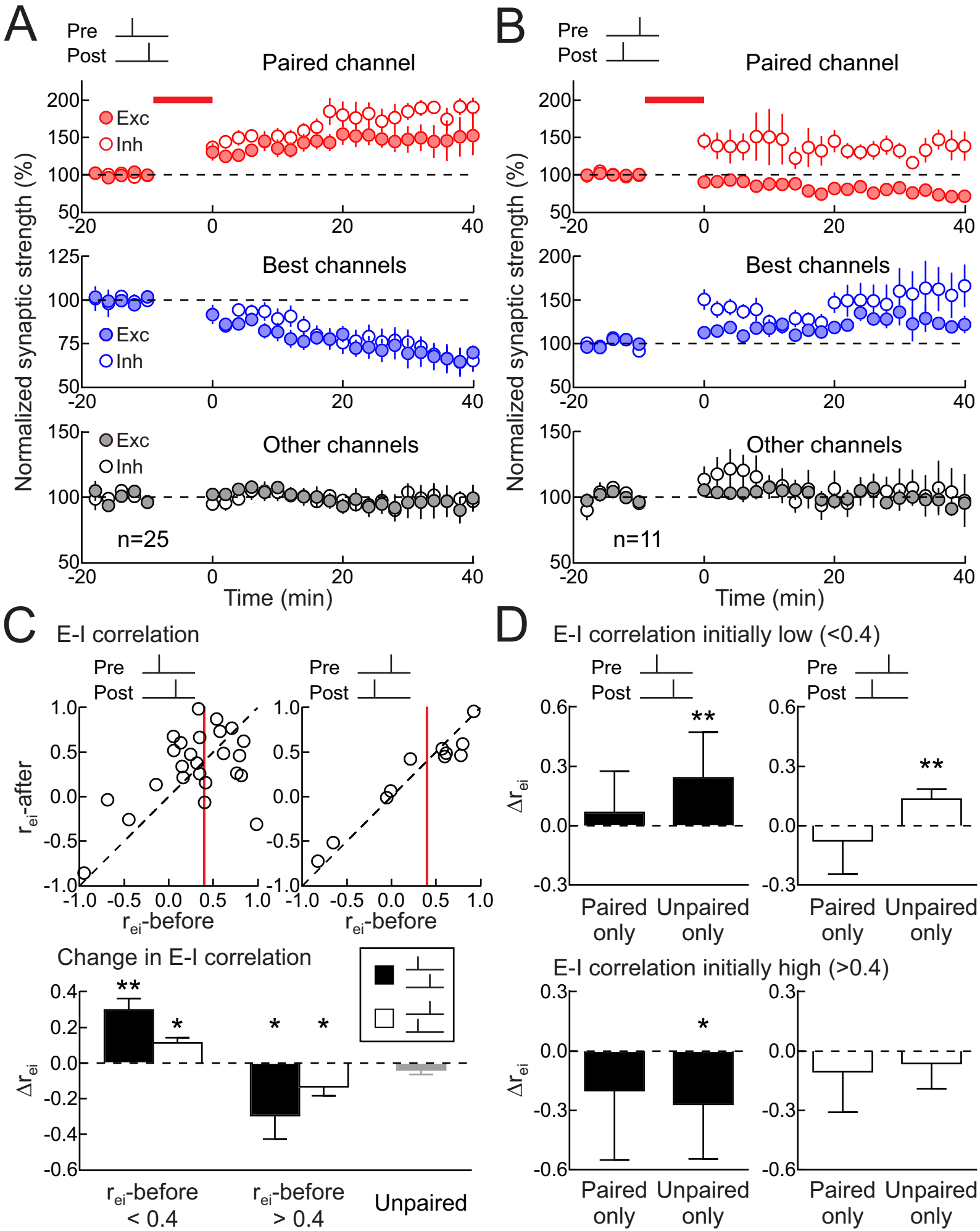
A
Pre
Post
Paired channel
Exc
Inh
Best channels
Exc
Inh
Other channels
Exc
Inh
n=25
Normalized synaptic strength (%)
Time (min)
B
Pre
Post
Paired channel
Best channels
Other channels
n=11
Normalized synaptic strength (%)
Time (min)
C
E-I correlation
Pre
Post
r_{ei}-after
r_{ei}-before
Change in E-I correlation
Δr_{ei}
r_{ei}-before < 0.4
r_{ei}-before > 0.4
Unpaired
D
E-I correlation initially low (<0.4)
Pre
Post
Δr_{ei}
Paired only
Unpaired only
E-I correlation initially high (>0.4)

Figure 2

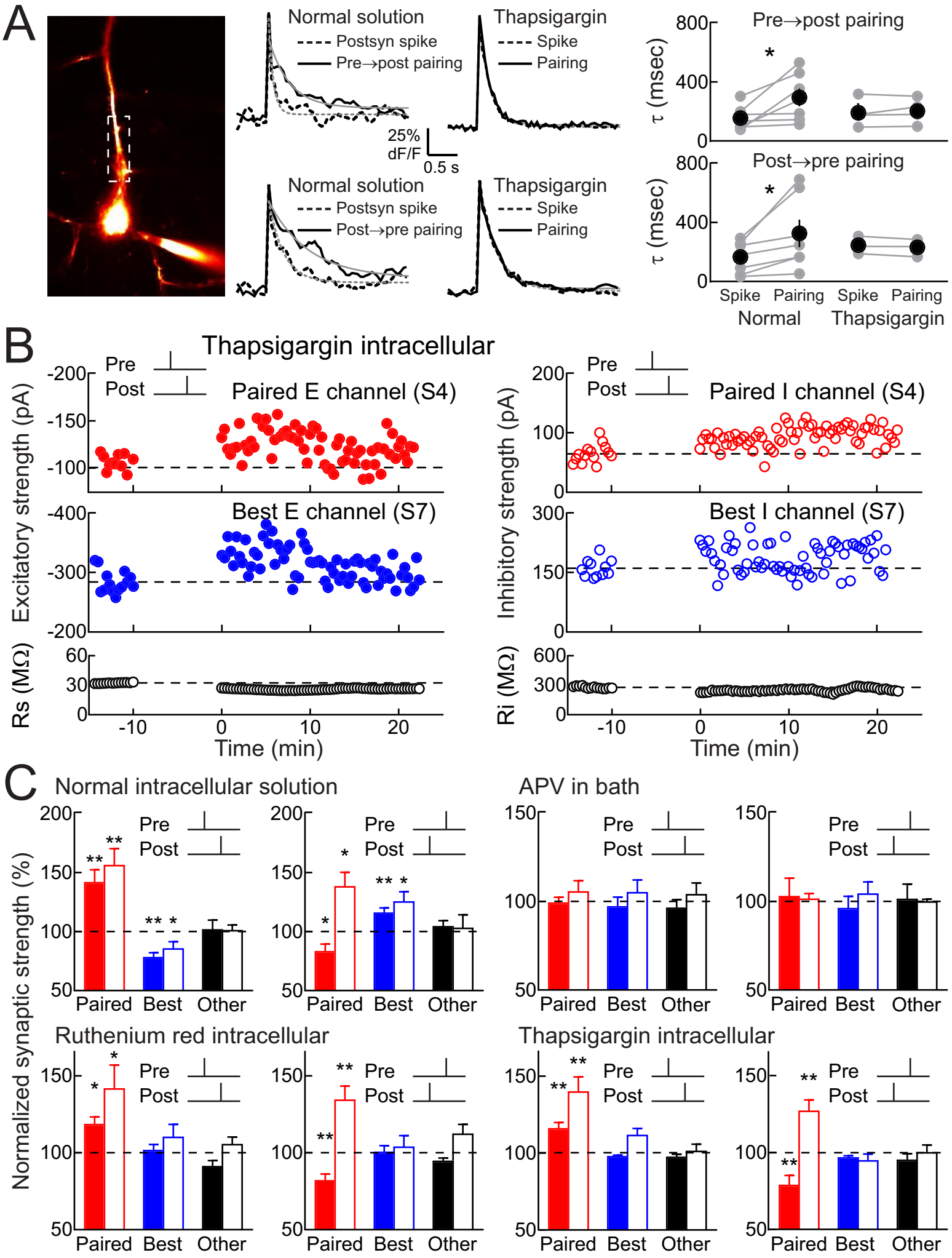
A
Normal solution
Postsyn spike
Pre→post pairing
Thapsigargin
Spike
Pairing
25% dF/F
0.5 s
Normal solution
Postsyn spike
Post→pre pairing
Thapsigargin
Spike
Pairing
Pre→post pairing
Post→pre pairing
τ (msec)
800
400
0
Spike
Pairing
Spike
Pairing
Normal
Thapsigargin
B
Thapsigargin intracellular
Pre
Post
Paired E channel (S4)
Best E channel (S7)
Paired I channel (S4)
Best I channel (S7)
Excitatory strength (pA)
Inhibitory strength (pA)
Rs (MΩ)
Ri (MΩ)
Time (min)
C
Normal intracellular solution
APV in bath
Ruthenium red intracellular
Thapsigargin intracellular
Normalized synaptic strength (%)
Paired
Best
Other

Figure 3

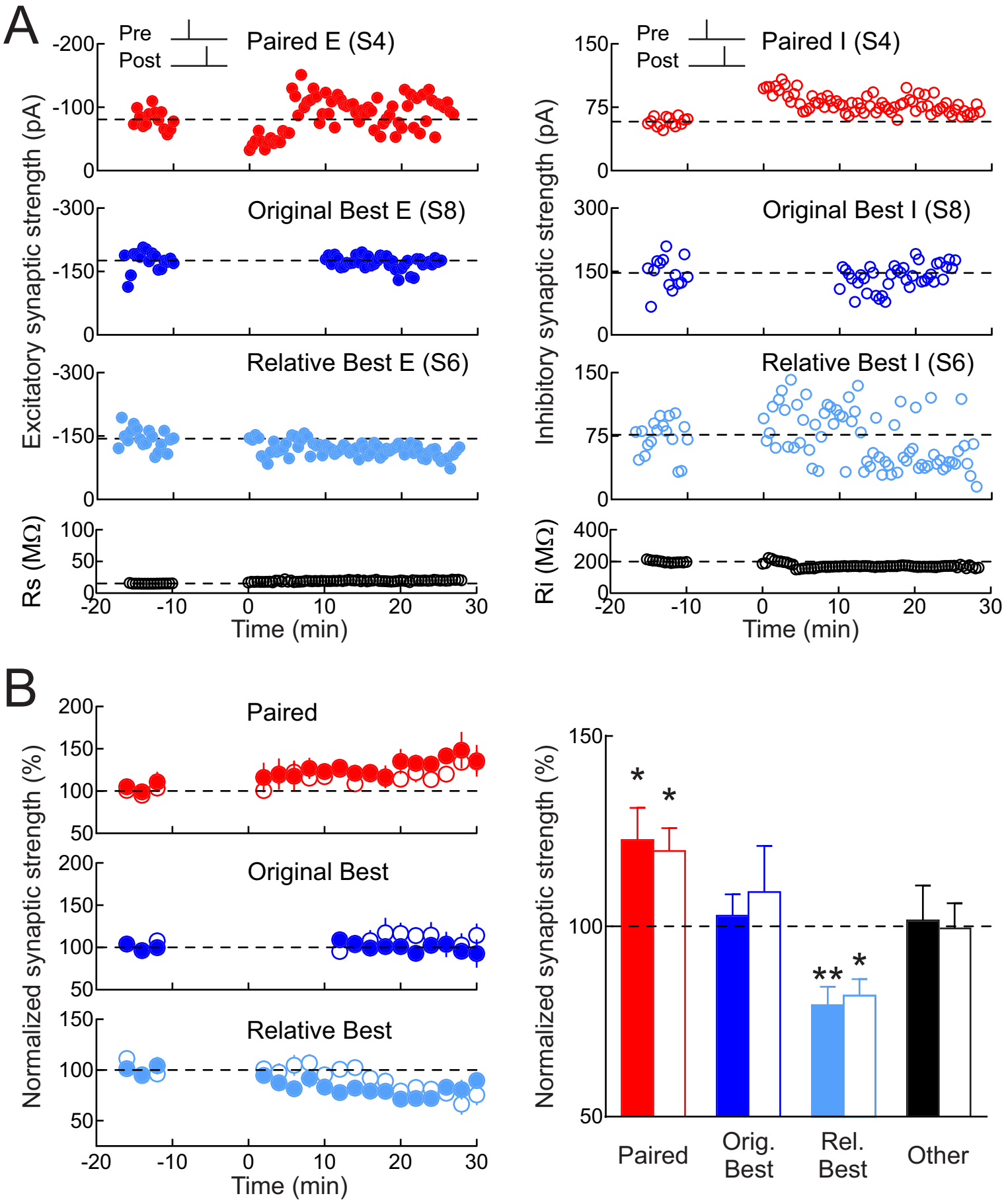
A
Pre
Post
Paired E (S4)
Original Best E (S8)
Relative Best E (S6)
Excitatory synaptic strength (pA)
Rs (MΩ)
Time (min)
Paired I (S4)
Original Best I (S8)
Relative Best I (S6)
Inhibitory synaptic strength (pA)
Ri (MΩ)
B
Paired
Original Best
Relative Best
Normalized synaptic strength (%)
Paired
Orig. Best
Rel. Best
Other

Figure 4

Supplementary Materials for

Heterosynaptic Plasticity Normalizes Cortical Excitatory-Inhibitory Balance

Authors: Rachel E. Field[1-4]†, James A. D'amour[1-4]†, Robin Tremblay[2,4,5], Bernardo Rudy[2,4,5], and Robert C. Froemke[1-4,6,7]*

Correspondence to: robert.froemke@med.nyu.edu

This PDF file includes:

Materials and Methods
Figs. S1 to S4

Materials and Methods

All procedures were approved under NYU School of Medicine IACUC protocols.

Slice preparation- mouse auditory cortex

Acute slices of auditory cortex were prepared from P9-35 C57Bl/6 mice, an age range spanning the critical period for excitatory-inhibitory balancing in rodent auditory cortex (7,13). Animals were deeply anesthetized with a 1:1 ketamine/xylazine cocktail and decapitated. The brain was rapidly placed in ice-cold dissection buffer containing (in mM): 87 NaCl, 75 sucrose, 2 KCl, 1.25 NaH_2PO_4, 0.5 $CaCl_2$, 7 $MgCl_2$, 25 $NaHCO_3$, 1.3 ascorbic acid, and 10 dextrose, bubbled with 95%/5% O_2/CO_2 (pH 7.4). Slices (300–400 µm thick) were prepared with a vibratome (Leica), placed in warm dissection buffer (33-35°C) for <30 min, then transferred to a holding chamber containing artificial cerebrospinal fluid at room temperature (ACSF, in mM: 124 NaCl, 2.5 KCl, 1.5 $MgSO_4$, 1.25 NaH_2PO_4, 2.5 $CaCl_2$, and 26 $NaHCO_3$,). Slices were kept at room temperature (22-24°C) for at least 30 minutes before use. For experiments, slices were transferred to the recording chamber and perfused (2–2.5 ml min^{-1}) with oxygenated ACSF at 33°C.

Electrophysiology

Somatic whole-cell recordings were made from layer 5 pyramidal cells in current-clamp and voltage-clamp mode with a Multiclamp 700B amplifier (Molecular Devices) using IR-DIC video microscopy (Olympus). Patch pipettes (3-8 MΩ) were filled with intracellular solution (in mM: 135 K-gluconate, 5 NaCl, 10 HEPES, 5 MgATP, 10 phosphocreatine, and 0.3 GTP. For pharmacological studies of **Figure 3**, either thapsigargin (10 µM) or

ruthenium red (20 μM) was included in the internal solution; in one experiment 1 μM thapsigargin was applied in the bath solution instead. Mean resting potential was –69.3±5.2 mV (standard deviation, SD), series resistance (Rs) was 17.4±11.9 MΩ, and the mean input resistance (Ri) was 238.1±96.2 MΩ, determined by monitoring cells with hyperpolarizing pulses (50 pA or 5-10 mV for 100 msec). Recordings were excluded from analysis if R_i changed >30% compared to the baseline period. Data were filtered at 2 kHz, digitized at 10 kHz, and analyzed with Clampfit 10 (Molecular Devices). Focal extracellular stimulation (0.033-0.2 Hz) was applied with a monopolar metal electrode 8-channel array (AMPI Master-9, stimulation strengths of 0-10 V for 6-30 μsec) located 100-150 μm from the recording electrode. Cells were held in voltage-clamp at two membrane potentials alternating between –40 mV to measure IPSCs and –80 mV to measure EPSCs. Mean peak EPSC (2 msec window) was used to measure excitatory strength. For IPSCs, a larger window (5-20 msec) was used. Stable baselines of synaptic strength were established by 5-20 min of stimulation. Synaptic strength after induction was measured 16-25 min after the end of the induction protocol. During induction, postsynaptic spiking was evoked with brief depolarizing current pulses. Presynaptic spike timing was defined as EPSP onset, and postsynaptic spike timing was measured at the peak of the action potential. All statistics and error bars are reported as means±SEM and statistical significance assessed with paired two-tailed Student's t-test, unless otherwise noted.

Two-photon Ca^{2+} imaging

Whole-cell recordings were performed with current-clamp intracellular solution containing Alexa Fluor (100 μM) to visualize the dendritic arbor and Fluo-4 (100-200 μM) to monitor

Ca^{2+} signals. In some experiments, thapsigargin (10 μM) was also added to the internal solution. Ca^{2+} imaging began at least 30 min after breakin to allow for dye diffusion, equilibration, and assess stability of the recording. Two-photon laser scanning microscopy of Ca^{2+} signals was performed using an upright microscope (BX61WI, Olympus), equipped with a slice recording chamber, 40X, 0.8 NA water immersion objective and a Ti:Sapphire (MaiTai DeepSee, Spectra-Physics, Mountain View, CA) laser tuned to 810 nm to excite both Alexa Fluor 594 and Fluo-4. Imaging of dendritic segments was acquired with Fluoview software (Olympus) at 4X digital zoom, every 50 ms. Images were analyzed in ImageJ (NIH, Bethesda, MD, USA).

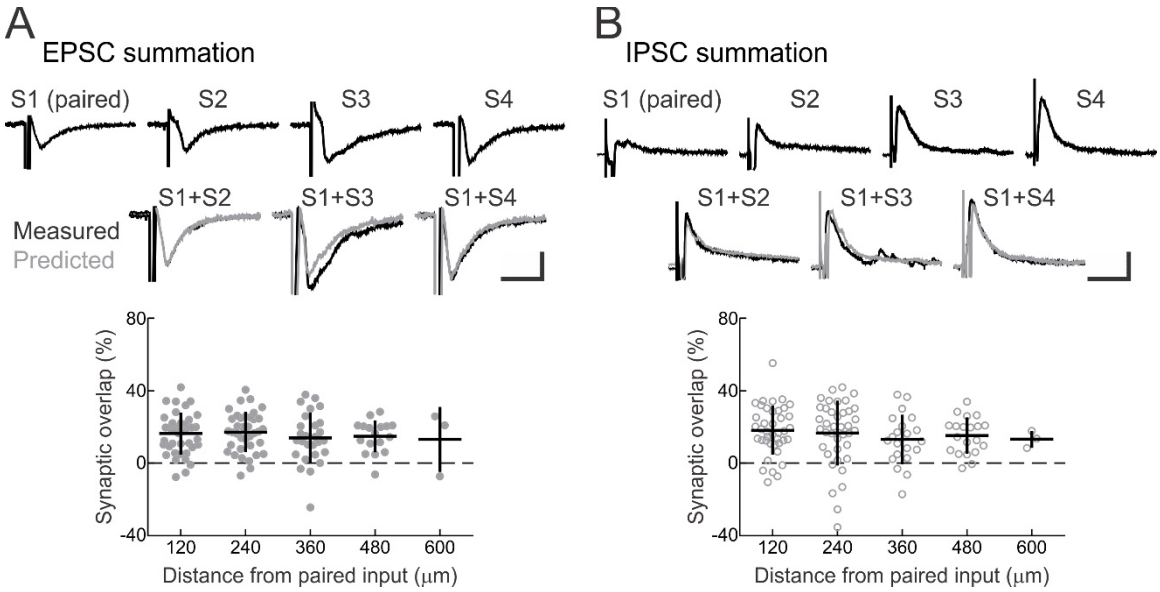

Fig. S1.

Assessment of synaptic overlap between different stimulation channels in auditory cortical slices.

(**A**) EPSC summation across channels. Top, example traces for one recording; there were four active stimulation electrodes (S1-S4), and S1 was the paired channel. Activating S1 together with either S2, S3, or S4 showed that approximately linear summation of EPSC pairs, indicating minimal overlap between excitatory inputs activated by S1 and S2, S3, or S4. Bottom, summary of channel overlap percentage across all cells with channel separation of 120 µm; overlap of 0% indicates independent summation (120 µm from paired channel: 16.5±11.7% overlap, mean±SD, n=40; 240 µm from paired channel: 17.2±11.1% overlap, n=37; 360 µm from paired channel: 13.9±14.0% overlap, n=27; 480 µm from paired channel: 14.9±8.9% overlap, n=17; 600 µm from paired channel: 13.2±18.0% overlap, n=3).

(**B**) IPSC summation across channels. Top, example traces from same cell as in **A**, showing IPSCs evoked by stimulation of the four active channels. Bottom, summary of IPSC

overlap across channels (120 µm from paired channel: 18.2±13.6% overlap, n=40; 240 µm from paired channel: 16.7±18.0% overlap, n=39; 360 µm from paired channel: 13.1±13.7% overlap, n=21; 480 µm from paired channel: 15.3±10.1% overlap, n=20; 600 µm from paired channel: 13.2±4.8% overlap, n=3).

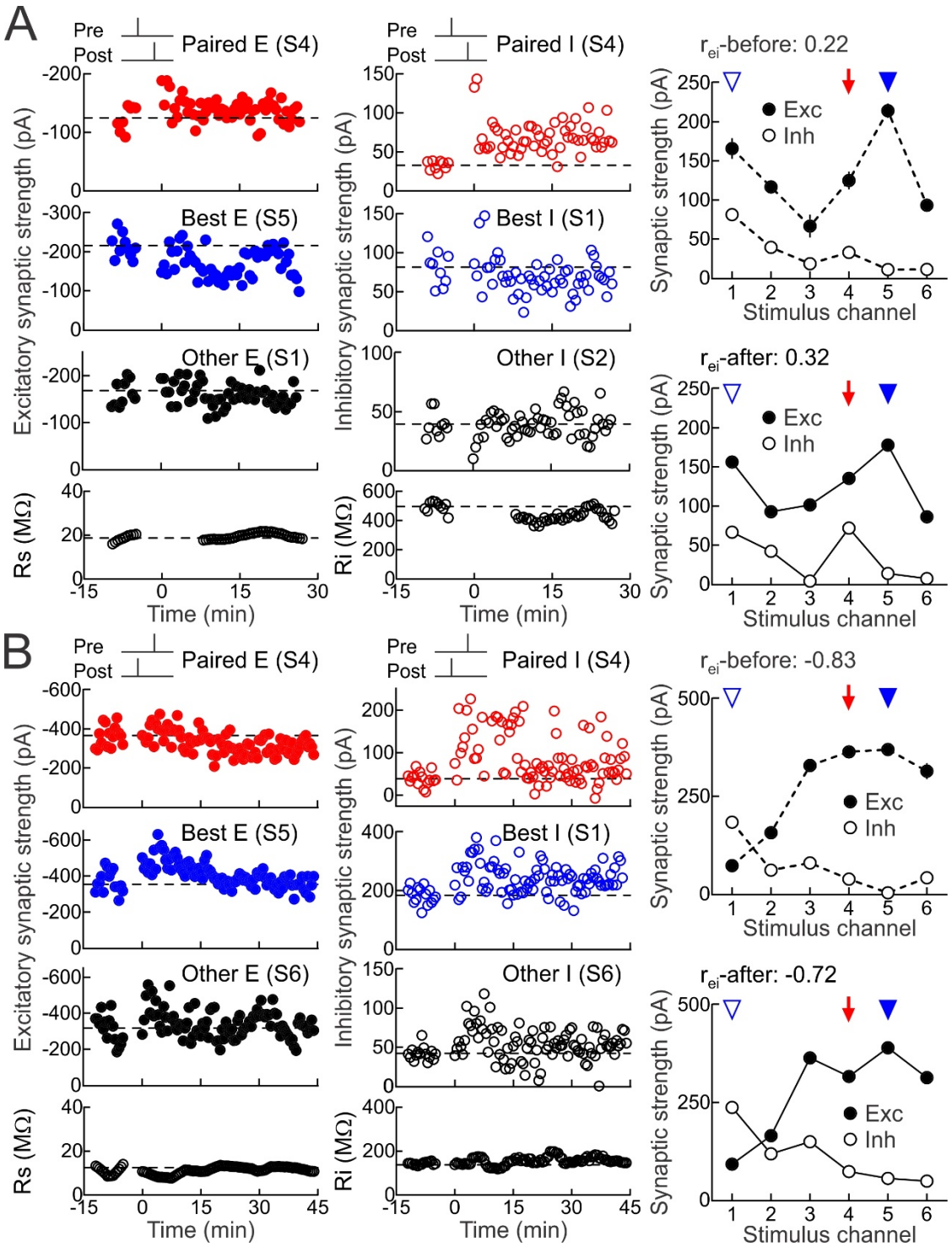

Fig. S2.

Examples of paired and heterosynaptic STDP increasing excitatory-inhibitory correlation when initially low.

(**A**) Example of excitatory and inhibitory plasticity induced by pre→post pairing at channel S4 (red, *Δt*: 4 msec; EPSCs before pairing: –124.8±7.5 pA; EPSCs after pairing: –135.2±4.4 pA, increase of 8.3%; IPSCs before pairing: 32.7±2.0 pA; IPSCs after pairing: 71.7±2.4 pA, increase of 119.2%). Dashed line, pre-pairing mean. Upper middle, heterosynaptic LTD at the strongest unpaired inputs onto this cell (blue, EPSCs at best channel S5 before: –214.2±9.8 pA, EPSCs after: –178.0±7.0 pA, decrease of –16.9%; IPSCs at best channel S1 before: 81.3±7.7 pA, IPSCs after: 66.4±4.0 pA, decrease of –18.4%). Lower middle, example other inputs (black, EPSCs at channel S1 before: –165.9±8.4 pA, EPSCs after: –156.2±4.3 pA, decrease of –5.8%; IPSCs at channel S2 before: 39.3±3.6 pA, IPSCs after: 42.1±3.2 pA, increase of 7.1%). Bottom, series and input resistances were stable (Rs before: 19.0±0.5 MΩ, Rs after: 20.7±0.2 MΩ, increase of 9.0%; Ri before: 496.8±11.2 MΩ, Ri after: 448.9±7.4 MΩ, decrease of –9.6%). Right, increase in excitatory-inhibitory correlation across all channels (r_{ei}-before: 0.22; r_{ei}-after: 0.32). Red arrow, paired channel. Blue arrowheads, original best excitation (filled) and inhibition (open).

(**B**) Example of plasticity induced by post→pre pairing at channel S4 (red, *Δt*: –4 msec; EPSCs before pairing: –363.8±14.2 pA; EPSCs after pairing: –316.7±11.9 pA, decrease of –12.9%; IPSCs before pairing: 38.4±4.3 pA; IPSCs after pairing: 72.9±13.2 pA, increase of 89.7%). Upper middle, heterosynaptic LTP at the strongest unpaired inputs onto this cell (blue, EPSCs at best channel S5 before: –370.1±15.6 pA, EPSCs after: –390.2±11.4 pA, increase of 5.4%; IPSCs at best channel S1 before: 183.9±7.4 pA, IPSCs after: 237.1±10.4 pA, increase of 28.9%). Lower middle, example other inputs (black, EPSCs at channel S6 before: –314.7±20.3 pA, EPSCs after: –313.7±15.6 pA, decrease of –0.3%; IPSCs at

channel S6 before: 41.8±2.2 pA, IPSCs after: 48.7±5.0 pA, increase of 16.5%). Bottom, series and input resistances were stable (Rs before: 10.9±0.5 MΩ, Rs after: 12.5±0.2 MΩ, increase of 15.0%; Ri before: 143.8±1.6 MΩ, Ri after: 161.4±2.8 MΩ, increase of 12.3%). Right, increase in excitatory-inhibitory correlation across all channels (r_{ei}-before: –0.83; r_{ei}-after: –0.72).

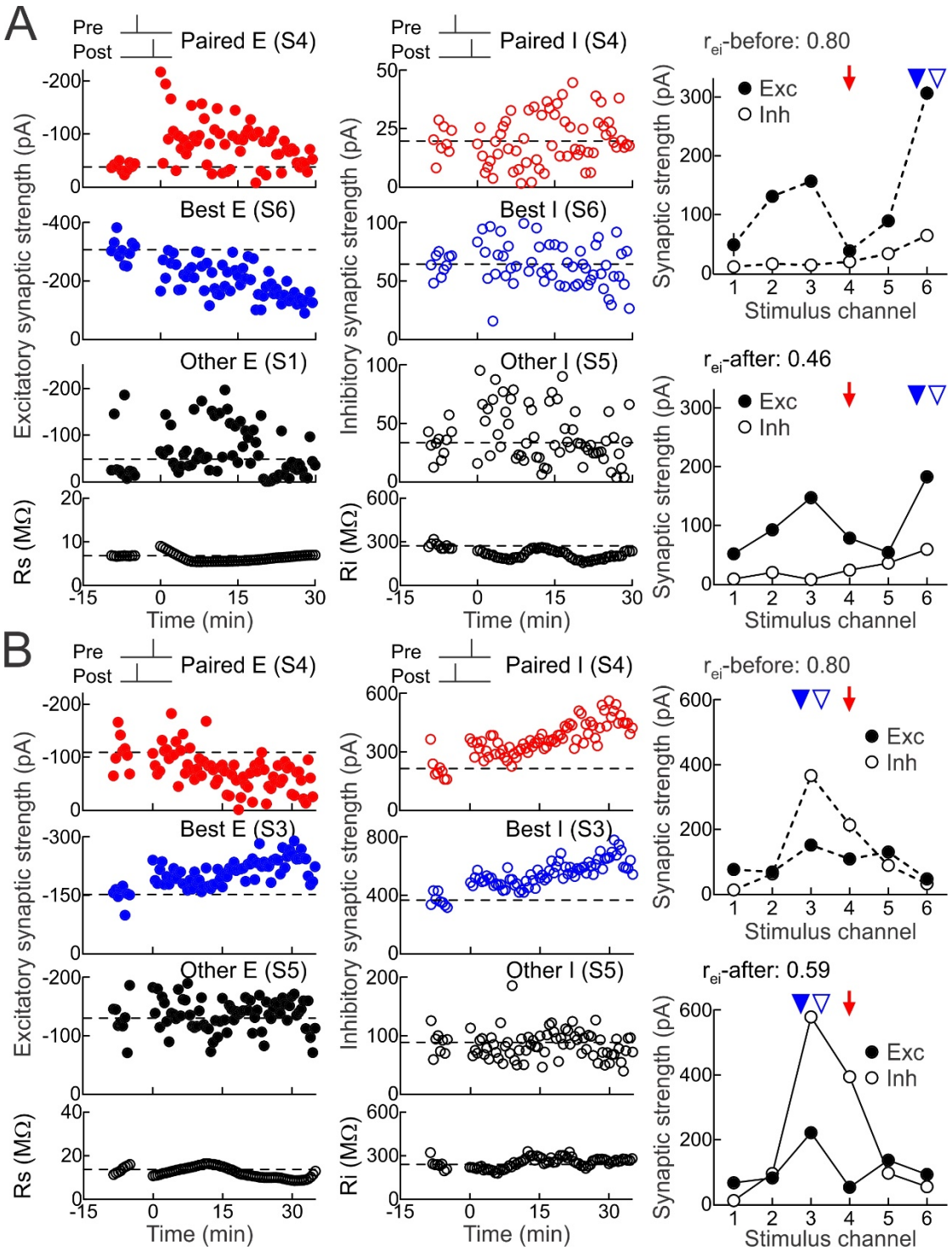

Fig. S3.

Examples of paired and heterosynaptic STDP decreasing excitatory-inhibitory correlation when initially high.

(**A**) Example of excitatory and inhibitory plasticity induced by pre→post pairing at channel S4 (red, *Δt*: 4 msec; EPSCs before pairing: –38.0±2.6 pA; EPSCs after pairing: –78.3±7.1 pA, increase of 105.9%; IPSCs before pairing: 19.7±2.4 pA; IPSCs after pairing: 23.8±2.4 pA, increase of 20.8%). Upper middle, heterosynaptic LTD at the strongest unpaired inputs onto this cell (blue, EPSCs at best channel S6 before: –306.5±12.4 pA, EPSCs after: –182.6±11.0 pA, decrease of –40.4%; IPSCs at best channel S6 before: 64.4±3.1 pA, IPSCs after: 59.3±3.9 pA, decrease of –7.9%). Lower middle, example other inputs (black, EPSCs at channel S1 before: –48.6±19.9 pA, EPSCs after: –51.5±10.6 pA, increase of 6.1%; IPSCs at channel S5 before: 33.5±4.1 pA, IPSCs after: 35.8±4.0 pA, increase of 6.8%). Bottom, series and input resistances were stable (Rs before: 6.8±0.02 MΩ, Rs after: 6.0±0.1 MΩ, decrease of –11.2%; Ri before: 272.4±6.5 MΩ, Ri after: 193.4±6.3 MΩ, decrease of –28.9%). Right, decrease in excitatory-inhibitory correlation across all channels (r_{ei}-before: 0.80; r_{ei}-after: 0.46). Red arrow, paired channel. Blue arrowheads, original best excitation (filled) and inhibition (open).

(**B**) Example of plasticity induced by post→pre pairing at channel S4 (red, *Δt*: –5 msec; EPSCs before pairing: –108.9±12.1 pA; EPSCs after pairing: –52.9±6.6 pA, decrease of –51.4%; IPSCs before pairing: 214.3±23.7 pA; IPSCs after pairing: 394.8±12.4 pA, increase of 84.2%). Upper middle, heterosynaptic LTP at the strongest unpaired inputs onto this cell (blue, EPSCs at best channel S3 before: –151.8±8.2 pA, EPSCs after: –222.0±5.0 pA, increase of 46.2%; IPSCs at best channel S3 before: 366.6±15.6 pA, IPSCs after: 580.2±9.9 pA, increase of 58.3%). Lower middle, example other inputs (black, EPSCs at channel S5 before: –130.0±11.7 pA, EPSCs after: –136.6±5.0 pA, increase of 5.1%; IPSCs at channel S5 before: 88.8±7.4 pA, IPSCs after: 96.7±3.9 pA, increase of 8.9%). Bottom,

series and input resistances were stable (Rs before: 13.7±0.6 MΩ, Rs after: 11.3±0.3 MΩ, decrease of –17.8%; Ri before: 240.1±13.2 MΩ, Ri after: 263.5±6.5 MΩ, increase of 9.7%). Right, decrease in excitatory-inhibitory correlation across all channels (r_{ei}-before: 0.80; r_{ei}-after: 0.59).

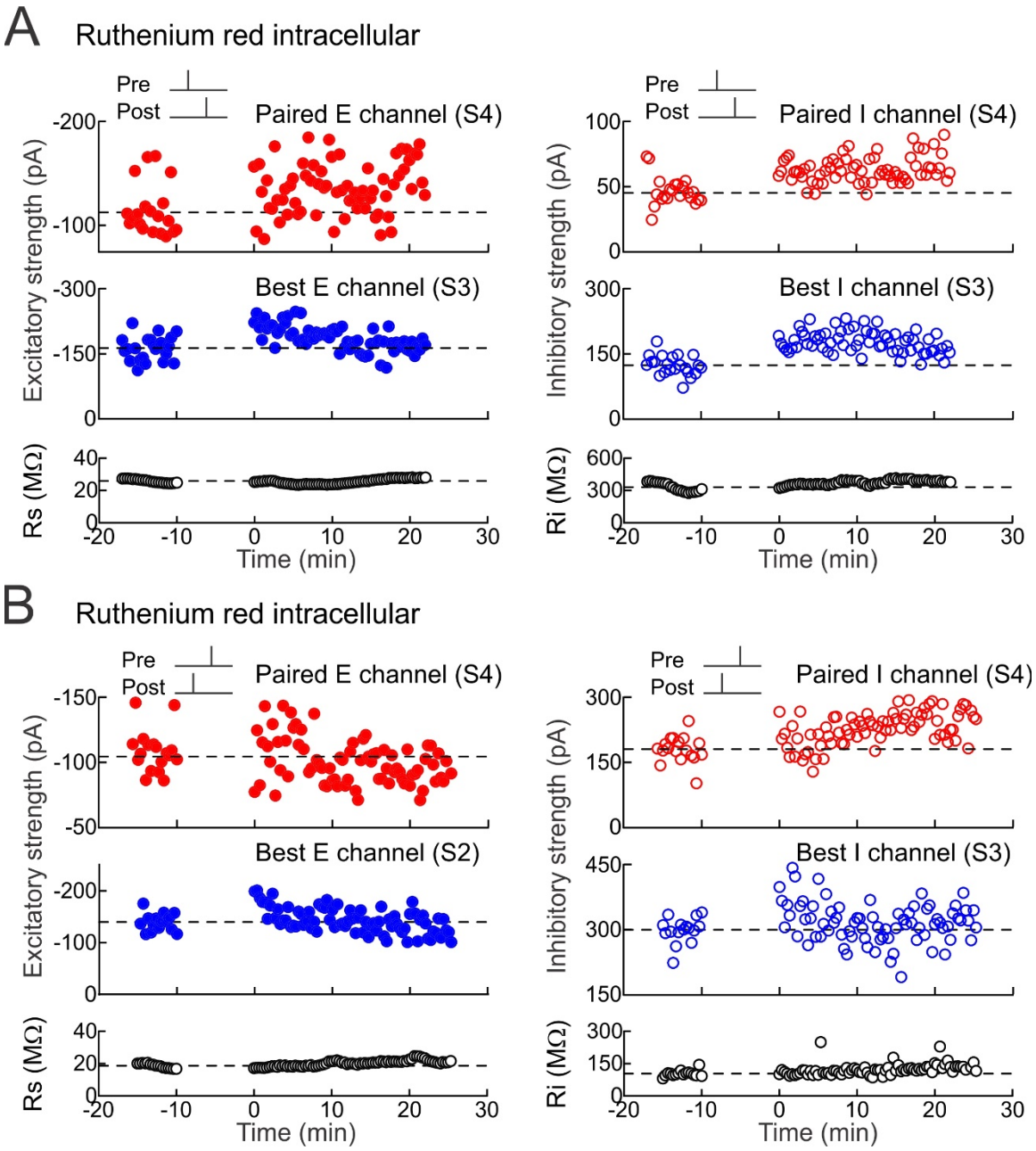

Fig. S4.

Intracellular blockade of Ca^{2+} store signaling with ruthenium red prevents heterosynaptic changes at the best inputs but spares STDP at paired inputs.

(**A**) Ruthenium red in the whole-cell pipette (20 µM) prevents heterosynaptic excitatory and inhibitory LTD after pre→post pairing. Top, example of excitatory LTP (left) and

inhibitory LTP (right) induced by pre→post pairing at channel S4 (red, Δt=1 msec; EPSCs before pairing: −112.6±5.8 pA, EPSCs after pairing: −143.3±6.3 pA, increase of 27.3%; IPSCs before pairing: 45.2±2.0 pA, IPSCs after pairing: 67.8±2.7 pA, increase of 49.9%). Dashed line, pre-pairing mean. Middle, ruthenium red prevented heterosynaptic LTD at the strongest unpaired inputs onto this cell (blue, EPSCs at channel S3 before: −163.1±6.1 pA, EPSCs after: −167.2±5.0 pA, increase of 2.5%; IPSCs at channel S3 before: 123.9±4.9 pA, IPSCs after: 164.3±4.9 pA, increase of 32.6%). Bottom, series and input resistance were stable (Rs before: 25.9±0.6 MΩ, Rs after: 27.6±0.3 MΩ, increase of 7.0%; Ri before: 330.4±20.7 MΩ, Ri after: 405.3±22.2 MΩ, increase of 13.8%).

(**B**) Ruthenium red prevents heterosynaptic excitatory and inhibitory LTP after post→pre pairing. Top, example of excitatory LTD (left) and inhibitory LTP (right) induced by post→pre pairing at channel S4 (red, Δt=−2 msec; EPSCs before pairing: −108.6±3.9 pA, EPSCs after pairing: −93.8±2.1 pA, decrease of −13.7%; IPSCs before pairing: 180.3±7.2 pA, IPSCs after pairing: 249.1±6.3 pA, increase of 38.1%). Middle, ruthenium red prevented heterosynaptic LTP at the strongest unpaired inputs onto this cell (blue, EPSCs at channel S2 before: −139.7±4.3 pA, EPSCs after: −132.4±4.1 pA, decrease of −5.2%; IPSCs at channel S3 before: 299.2±7.3 pA, IPSCs after: 318.9±6.9 pA, increase of 6.6%). Bottom, series and input resistance were stable (Rs before: 18.7±0.4 MΩ, Rs after: 21.8±0.2 MΩ, increase of 16.9%; Ri before: 103.6±3.4 MΩ, Ri after: 147.6±13.6 MΩ, increase of 13.6%).